Supplementary Information of

Atmospheric particle abundance and sea salt aerosol observations in the springtime Arctic: a focus on blowing snow and leads

Qianjie Chen[1,10], Jessica A. Mirrielees[1], Sham Thanekar[2], Nicole A. Loeb[3,12], Rachel M. Kirpes[1], Lucia M. Upchurch[4,5], Anna J. Barget[1], Nurun Nahar Lata[6], Angela R. W. Raso[1,7], Stephen M. McNamara[1], Swarup China[6], Patricia K. Quinn[4], Andrew P. Ault[1], Aaron Kennedy[3], Paul B. Shepson[7,8,11], Jose D. Fuentes[2], and Kerri A. Pratt[1,9]

[1] Department of Chemistry, University of Michigan, Ann Arbor, Michigan 48109, United States
[2] Department of Meteorology and Atmospheric Science, Pennsylvania State University, University Park, Pennsylvania 16801, United States
[3] Department of Atmospheric Sciences, University of North Dakota, Grand Forks, North Dakota 58202, United States
[4] Pacific Marine Environmental Laboratory, National Oceanic and Atmospheric Administration, Seattle, Washington 98115, United States
[5] Cooperative Institute for Climate, Ocean, and Ecosystem Studies, University of Washington, Seattle, Washington 98115, United States
[6] Environmental Molecular Sciences Laboratory, Pacific Northwest National Laboratory, Richland, Washington 99352, United States
[7] Department of Chemistry, Purdue University, West Lafayette, Indiana 47907, United States
[8] Department of Earth, Atmospheric, and Planetary Sciences & Purdue Climate Change Research Center, Purdue University, West Lafayette, Indiana 47907, United States
[9] Department of Earth and Environmental Sciences, University of Michigan, Ann Arbor, Michigan 48109, United States
[10] Now at Department of Civil and Environmental Engineering, The Hong Kong Polytechnic University, Hong Kong SAR, China
[11] Now at School of Marine and Atmospheric Sciences, Stony Brook University, Stony Brook, New York 11794, United States
[12] Now at Department of Environment and Geography, University of Manitoba, Winnipeg, Manitoba, Canada

Correspondence to: Kerri A. Pratt (prattka@umich.edu)

Supplementary Information

Text S1 provides supplementary results and discussion of the chemical composition of atmospheric particles during moderate wind speed periods, during observed and falsely predicted blowing snow periods, and regarding sea salt aerosol sources during observed blowing snow. The NOAA Barrow Observatory submicron and supermicron particle [NH_4^+], [NO_3^-], [Br^-], methanesulfonate ([MSA^-]), and oxalate mass concentration data are shown in Table S1 for the time periods of interest for reference. Submicron and supermicron particle [Na^+], [Cl^-], [SO_4^{2-}], [Ca^{2+}], [Mg^{2+}], and [K^+] mass

concentration data are shown in Table S2. Table S3 shows the $[Cl^-]/[Na^+]$, $[SO_4^{2-}]/[Na^+]$, $[Ca^{2+}][Na^+]$, $[Mg^{2+}]/[Na^+]$, and $[K^+]/[Na^+]$ molar ratios for submicron and supermicron particles, local tundra surface snowpack, and previous measurements of sea ice surface snowpack, blowing snow, frost flowers, and seawater. Figure S1 shows the time-resolved size distributions of ambient particles measured by an optical particle sizer (OPS) and a scanning mobility particle sizer (SMPS). The comparison of total particle number concentrations measured by SMPS and CPC is shown in Figure S2. The size-resolved numbers of particles measured by CCSEM-EDX for the four samples collected during this study are shown in Figure S3. The representative SEM images and EDX spectra of the main particle types observed are shown in Figure S4. Digital color histograms of the EDX spectra of individual 0.4-2.8 μm d_a fresh sea spray aerosol particles are shown in Figure S5.

S1. Additional results and discussion of the chemical composition of atmospheric particles

S1.1 Moderate wind speed periods

In this study, individual dust (mainly aluminum and silicon-containing, with some calcium), soot, and potassium+sulfur (presumably in the form of sulfate) aerosol particles comprised 0-31%, 0-15%, and 0-6%, by number, respectively, across the 0.09-0.9 μm d_{pa} range (d_a 0.07-0.4 μm impactor stage) on April 15-16 (Fig. 6a). During April 15-16, submicron particle non-sea-salt calcium, magnesium, and potassium mole fractions ($f_{\mathrm{nssCa^{2+}}}$, $f_{\mathrm{nssMg^{2+}}}$, and $f_{\mathrm{nssK^{+}}}$) were calculated to be 77%, 25%, and 78%, respectively, consistent with the observed submicron dust and potassium+sulfur aerosol particles. Similar to the low wind periods, the submicron particle $[K^+]/[Na^+]$ (average 0.09±0.05 mol mol^{-1}) and $[Ca^{2+}]/[Na^+]$ (average 0.08±0.03 mol mol^{-1}) were higher than those of seawater (both 0.02 mol mol^{-1}; Millero et al., 2008) during moderate wind periods (Fig. 5), consistent with contributions from long-range transported aerosols during springtime Arctic haze in Utqiaġvik (Quinn et al., 2002; 2007).

Note that Mg was also enriched (Mg/Na = 0.6±0.3 during April 15-16; 0.5±0.2 during April 16) in the 0.07-0.4 μm d_a individual sea spray aerosol particles (Table 3), compared to seawater (0.11; Millero et al., 2008). This divalent cation binds with organic matter (exopolymeric substances; Krembs et al., 2002) within the sea surface microlayer, resulting in magnesium-enriched organic coatings on the sea salt aerosol (Jayarathne et al., 2016; Bertram et al., 2018; Kirpes et al., 2019).

Individual potassium chloride and mineral dust particles accounted for 67±8%, and 3±2%, on average by number, respectively, of the particles, respectively, collected during April 15-16 and April 16 on the 0.4-2.8 μm d_a impactor stage. For the April 28 – May 4 supermicron particle sample, the non-sea-salt mole fractions of calcium ($f_{\mathrm{nssCa^{2+}}} = \frac{\mathrm{Total\ Ca^{2+}} - 0.02\mathrm{Na^{+}}}{\mathrm{Total\ Ca^{2+}}}$, Quinn et al. (2002)), magnesium ($f_{\mathrm{nssMg^{2+}}} = \frac{\mathrm{Total\ Mg^{2+}} - 0.11\mathrm{Na^{+}}}{\mathrm{Total\ Mg^{2+}}}$), and potassium ($f_{\mathrm{nssK^{+}}} = \frac{\mathrm{Total\ K^{+}} - 0.02\mathrm{Na^{+}}}{\mathrm{Total\ K^{+}}}$) were 88%, 51%, and 71%, respectively, consistent with the observed individual potassium chloride and mineral dust particles. For comparison, during April 28 – May 4, submicron particle $f_{\mathrm{nssCa^{2+}}}$, $f_{\mathrm{nssMg^{2+}}}$, and $f_{\mathrm{nss}\ +}$ were calculated to be 70±10%, 20±10%, and 80±10%, respectively.

For the individual sea spray aerosol particles collected on the 0.4-2.8 μm d_a stage, magnesium was enriched (average 0.40 ± 0.08) relative to seawater (Mg/Na ratio = 0.11) during April 15–16. Calcium was also enriched relative to seawater (Ca/Na ratio = 0.02) in these sea spray aerosol particles, with Ca/Na ratios of 0.06 ± 0.02 during April 1516 and 0.23 ± 0.08 during April 16, as previously observed in Arctic sea salt aerosol (Salter et al., 2016). As discussed above, these divalent cations bind with exopolymeric substances (Krembs et al., 2002) within the sea surface microlayer, resulting in enrichments in organic coatings of the sea spray aerosol (Jayarathne et al., 2016; Bertram et al., 2018; Kirpes et al., 2019).

S1.2 Observed and falsely predicted blowing snow periods

Mineral dust, soot, and potassium+sulfur aerosol particles comprised only 0-6%, 0-4%, and 0-2%, by number, respectively, across the 0.09-0.9 μm d_{pa} range (d_a 0.07-0.4 μm impactor stage) during the observed BLSN period (April 6-7), compared to 0-31%, 0-15%, and 0-6%, by number, respectively, during the moderate wind speed period of April 15-16. Similar to the moderate wind period samples, potassium chloride particles accounted for 47±8%, by number, and mineral dust accounted for 1±1% of the particles collected on the 0.4-2.8 μm d_a impactor stage during April 6 07:00–19:00.

Submicron particle [Ca^{2+}], [Mg^{2+}], and [K^{+}] also increased during observed BLSN periods (Fig. 4). The submicron particle $f_{\mathrm{nssCa^{2+}}}$, $f_{\mathrm{nssMg^{2+}}}$, and $f_{\mathrm{nssK^{+}}}$ were 44±11%, 1±4%, and 50±9%, respectively, during observed BLSN periods, suggesting

that nearly all of the observed Mg^{2+} and approximately half of the Ca^{2+} and K^+ were associated with sea salt aerosol. The remaining contributions are attributed to the mineral dust and potassium+sulfur particles. Supermicron particle [Ca^{2+}], [Mg^{2+}] and [K^+] were highest during April 7-13 (BLSN winds), lowest during April 28 – May 4 (NBLSN winds), and in between during April 14-20 and April 21-27, which experienced a range of wind speeds (Fig. 4).

S1.3 Sea salt aerosol sources during observed blowing snow

The average [Mg^{2+}]/[Na^+] molar ratio of the surface snowpack over Beaufort Sea first-year sea ice (0.1; Krnavek et al., 2012) is similar to that of seawater (0.11; Millero et al., 2008). In comparison, springtime blowing snow collected over Utqiaġvik tundra was previously observed to be enriched in magnesium (0.20±0.05; Jacobi et al., 2012). Submicron particles during observed BLSN and supermicron particles during observed + falsely predicted BLSN (April 7-13) showed magnesium enrichment, with [Mg^{2+}]/[Na^+] of 0.13±0.01 and 0.15, respectively (Fig. 5). The individual 0.07-0.40 µm d_a sea spray aerosol particles collected overnight from April 6 19:00 to April 7 07:00 also showed magnesium enrichment, with an average Mg/Na of 0.17±0.02 mol mol^{-1} (Table 3). The individual 0.4-2.8 µm d_a sea spray aerosol particles, collected during April 6 daytime showed significant magnesium enrichment of 0.34±0.03 (Mg/Na), similar to during the moderate wind conditions (0.40±0.08 and 1.2±0.4) (Table 3). Similar to the observed calcium enrichment, the magnesium enrichment in both the submicron and supermicron particles is likely due to sea spray aerosol organic coatings enriched in divalent cations, as found from bubble bursting (Kirpes et al., 2019; Jayarathne et al., 2016; Orellana and Leck, 2015; Salter et al., 2016). The brine of frost flowers is also enriched in magnesium ([Mg^{2+}]/[Na^+]=0.135±0.005 mol mol^{-1}, Douglas et al., 2012; 0.20±0.05, Jacobi et al., 2012), leading as speculated in a previous field study in Greenland by Hara et al. (2017) to speculate that the sublimation of blowing snow influenced by frost flower brine would also be enriched in magnesium, relative to seawater. However, frost flower brine influence would be expected to also lead to significant sulfate depletion, which was not observed, as discussed below (Table 3, Figure 5, and Table S3), suggesting contribution from bubble bursting sea spray aerosol production is most likely.

The [Mg^{2+}]/[Na^+] of the local tundra surface snowpack during observed BLSN periods was 0.07±0.01 mol mol^{-1}, lower than

that of seawater (0.11; Millero et al., 2008), the bulk submicron and supermicron aerosol, previous blowing snow observations, and previous first-year sea ice surface snow (Fig. 5), as discussed above. Krnavek et al. (2012) also found magnesium depletion in some of their springtime Utqiaġvik tundra surface snowpack samples. Notably, the individual 0.07-0.4 μm d_a sea spray aerosol particles collected on April 6 also showed magnesium depletion, with an average Mg/Na of 0.06±0.01 (Table 3). Of the seven individual particle sampling periods analyzed, this was the only period with magnesium depleted sea spray aerosol particle present. The reason for this observed magnesium depletion is not known. Conversely, the larger individual sea spray aerosol particles (0.4-2.8 μm d_a) collected during the same time period were enriched in magnesium, as discussed above (Table 3). The similarity between the local tundra surface snowpack and 0.07-0.4 μm d_a sea spray aerosol particle composition is notable. However, it should be noted that the observed individual sea spray aerosol particles were depleted in Cl and enriched in both S and Ca, in contrast to the tundra surface snowpack (Table 3 and Figure 5).

Table S1. The NH_4^+, NO_3^-, Br^-, MSA^-, and oxalate ($C_2O_4^{2-}$) mass concentrations (average ± 1σ) for daily submicron particle samples during observed BLSN, falsely predicted BLSN, moderate wind, and low wind periods, and for supermicron particles collected on April 7-13, April 14-20, April 21-27, and April 28-May 4. The limits of detection (LODs) were 0.0001 μg m^{-3}.

Sample type	Category	$[NH_4^+]$ (μg m^{-3})	$[NO_3^-]$ (μg m^{-3})	$[Br^-]$ (ng m^{-3})	$[MSA^-]$ (μg m^{-3})	Oxalate (μg m^{-3})
Submicron particles	Observed BLSN	0.21±0.05	0.03±0.01	1.8±0.8	0.002±0.002	0.009±0.002
	Falsely Predicted BLSN	0.22±0.05	0.021±0.008	2±1	0.003±0.003	0.009±0.003
	Moderate wind	0.23±0.09	0.02±0.01	2±1	0.007±0.006	0.008±0.003
	Low wind	0.2±0.1	0.020±0.009	1.2±0.6	0.008±0.006	0.006±0.002
Supermicron particles	04/7-13	< LOD	0.022	0.3	< LOD	0.0012
	04/14-20	< LOD	0.013	0.1	< LOD	0.0004
	04/21-27	< LOD	0.032	< LOD	0.0002	0.0015
	04/28-05/04	< LOD	0.008	0.1	0.0002	0.0010

Table S2. The Na^+, Cl^-, SO_4^{2-}, Ca^{2+}, Mg^{2+}, and K^+ concentrations (average ± 1σ) for daily submicron particle samples during observed BLSN, falsely predicted BLSN, moderate wind, and low wind periods, and for supermicron particles collected on April 7-13, April 14-20, April 21-27, and April 28-May 4. The submicron particle mass concentrations (average ± 1σ) during the four supermicron particle collection periods are also shown for comparison.

Sample type	Category	$[Na^+]$ ($\mu g\ m^{-3}$)	$[Cl^-]$ ($\mu g\ m^{-3}$)	$[SO_4^{2-}]$ ($\mu g\ m^{-3}$)	$[Ca^{2+}]$ ($\mu g\ m^{-3}$)	$[Mg^{2+}]$ ($\mu g\ m^{-3}$)	$[K^+]$ ($\mu g\ m^{-3}$)
Submicron particles	Observed BLSN	0.5±0.3	0.9±0.7	0.7±0.2	0.03±0.02	0.07±0.04	0.03±0.02
	Falsely Predicted BLSN	0.3±0.1	0.3±0.2	0.7±0.2	0.02±0.01	0.03±0.02	0.02±0.01
	Moderate wind	0.2±0.1	0.1±0.1	0.7±0.3	0.02±0.01	0.02±0.01	0.02±0.01
	Low wind	0.1±0.2	0.1±0.2	0.7±0.5	0.01±0.01	0.02±0.02	0.02±0.01
	04/7-13	0.3±0.2	0.5±0.4	0.6±0.1	0.020±0.009	0.05±0.02	0.02±0.01
	04/14-20	0.1±0.1	0.1±0.1	0.6±0.1	0.014±0.004	0.02±0.01	0.01±0.01
	04/21-27	0.3±0.1	0.3±0.1	1.0±0.3	0.022±0.004	0.04±0.01	0.03±0.01
	04/28-05/04	0.1±0.2	0.1±0.1	0.7±0.5	0.013±0.008	0.02±0.01	0.02±0.01
Supermicron particles	04/7-13	0.619	0.870	0.045	0.030	0.100	0.034
	04/14-20	0.083	0.133	0.019	0.006	0.012	0.004
	04/21-27	0.341	0.570	0.081	0.020	0.036	0.014
	04/28-05/04	0.017	0.014	0.018	0.005	0.004	0.002

Table S3. The $[Cl^-]/[Na^+]$, $[SO_4^{2-}]/[Na^+]$, $[Ca^{2+}][Na^+]$, $[Mg^{2+}]/[Na^+]$, and $[K^+]/[Na^+]$ molar ratios for submicron particles (average ± 1σ) and local tundra surface snowpack (average ± 1σ) for the categories of observed blowing snow (BLSN), falsely predicted BLSN, moderate wind, and low wind speeds. The corresponding data for the four supermicron particle samples is shown, with comparison to the average (± 1σ) for the submicron particle ion ratios during those periods. Comparison is shown to previous measurements of sea ice surface snowpack (Krnavek et al., 2012), blowing snow (Jacobi et al., 2012), frost flowers (Douglas et al., 2012), and seawater (Millero et al., 2008).

Sample type	Category	$[Cl^-]/[Na^+]$ (mol mol^{-1})	$[SO_4^{2-}]/[Na^+]$ (mol mol^{-1})	$[Ca^{2+}]/[Na^+]$ (mol mol^{-1})	$[Mg^{2+}]/[Na^+]$ (mol mol^{-1})	$[K^+]/[Na^+]$ (mol mol^{-1})
Submicron particles[1]	Observed BLSN	0.9±0.3	0.5±0.4	0.04±0.01	0.13±0.01	0.04±0.01
	Falsely predicted BLSN	0.8±0.2	0.8±0.4	0.05±0.02	0.13±0.01	0.05±0.01
	Moderate wind	0.5±0.2	1.4±0.6	0.08±0.03	0.14±0.05	0.09±0.05
	Low wind	0.4±0.2	1.6±0.7	0.08±0.03	0.11±0.05	0.15±0.08
	04/7-13	0.9±0.2	0.5±0.3	0.036±0.004	0.13±0.01	0.04±0.01
	04/14-20	0.6±0.2	1.5±0.6	0.09±0.03	0.18±0.04	0.08±0.03
	04/21-27	0.7±0.1	0.9±0.2	0.05±0.01	0.12±0.01	0.06±0.02
	04/28-05/04	0.3±0.2	1.6±0.6	0.07±0.02	0.14±0.02	0.11±0.06
Supermicron particles[1]	04/7-13	0.9	0.017	0.03	0.15	0.03
	04/14-20	1.0	0.056	0.04	0.14	0.03
	04/21-27	1.1	0.057	0.03	0.10	0.02
	04/28-05/04	0.6	0.261	0.16	0.23	0.08
Tundra surface snowpack[1]	Observed BLSN	1.1±0.1	0.04±0.01	0.033±0.004	0.07±0.01	0.019±0.004
	Falsely predicted BLSN	1.3±0.4	0.05±0.01	0.025±0.007	0.07±0.02	0.019±0.006
	Moderate wind	1.3±0.3	0.3±0.4	0.2±0.2	0.1±0.1	0.05±0.03
	Low wind	1.4±0.4	0.5±0.5	0.2±0.2	0.2±0.1	0.06±0.05
Sea ice surface snowpack[2]		1.2	0.04	0.02	0.10	0.02
Blowing snow[3]		1.21±0.07	0.03±0.01	0.06±0.02	0.20±0.05	0.022±0.003
Frost Flowers[4]		1.32±0.03	0.016±0.003	0.0216±0.0009	0.135±0.005	0.0239±0.0009
Seawater[5]		1.2	0.06	0.02	0.11	0.02

[1] This study [2] Krnavek et al. (2012) [3] Jacobi et al. (2012) [4] Douglas et al. (2012) [5] Millero et al. (2008)

Table S4. The Na^+, K^+, Ca^{2+}, Mg^{2+}, Cl^-, NO_3^-, Br^-, and SO_4^{2-} concentrations (average ± 1σ) for local tundra surface snowpack samples during observed BLSN, falsely predicted BLSN, moderate wind, and low wind periods.

Tundra snowpack	$[Na^+]$ (μM)	$[K^+]$ (μM)	$[Ca^{2+}]$ (μM)	$[Mg^{2+}]$ (μM)	$[Cl^-]$ (μM)	$[NO_3^-]$ (μM)	$[Br^-]$ (μM)	$[SO_4^{2-}]$ (μM)
Observed BLSN	194±57	4±2	6±2	13±6	218±67	4±2	0.2±0.2	8±3
Falsely Predicted BLSN	229±115	5±3	6±4	18±13	280±123	4±2	0.3±0.3	10±5
Moderate wind	151±144	4±3	6±3	14±15	175±168	7±4	0.5±0.3	12±5
Low wind	89±68	2±1	6±1	9±5	105±76	8±4	0.9±0.3	15±5

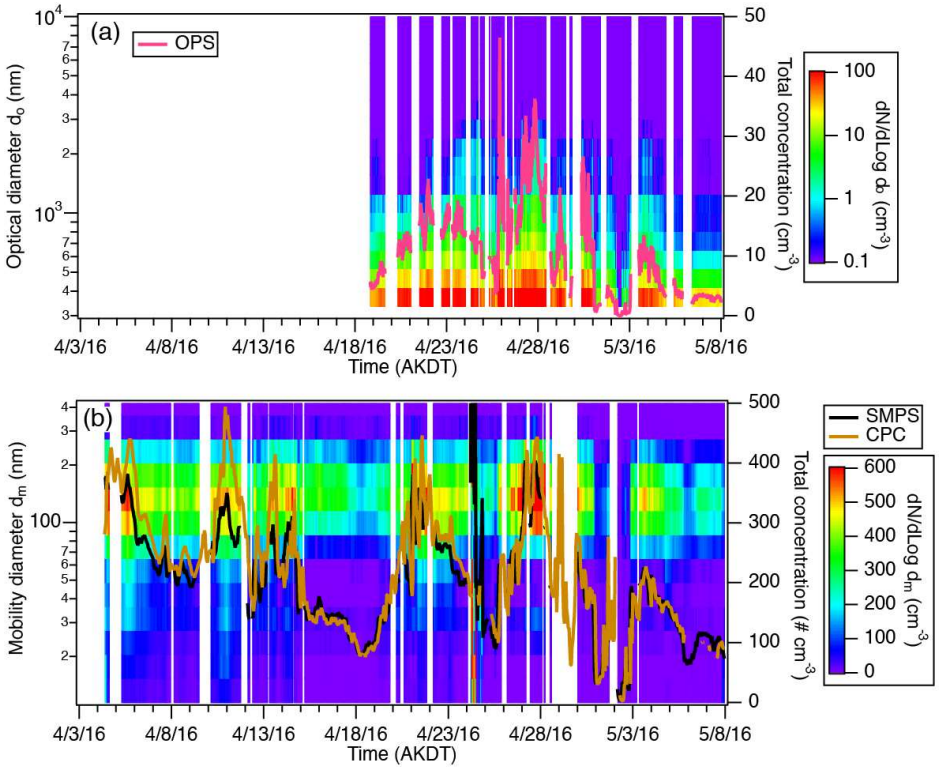

Figure S1. Time series of size distribution of ambient particles measured by (a) an optical particle sizer (OPS) and (b) a scanning mobility particle sizer (SMPS), and total number concentrations measured by the OPS, SMPS, and condensation particle sizer (CPC). Short spikes with total SMPS concentrations > 500 particles cm^{-3} lasting for < 20 minutes were likely

local combustion emission and were therefore removed for this data analysis. Spikes in total SMPS concentrations (> 2000 particles cm^{-3}) were observed frequently on April 24 due to nearby generator use, and therefore, this day was also removed for this data analysis.

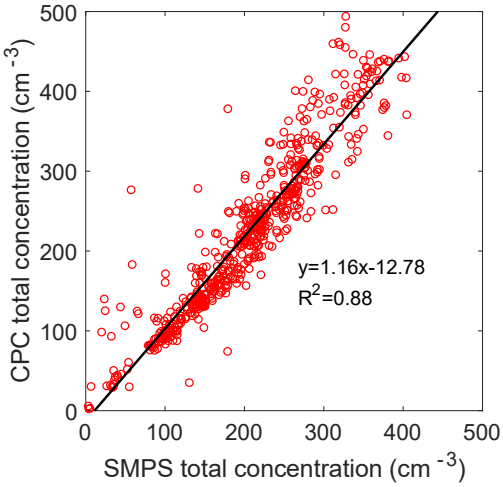

155

Figure S2. Comparison of hourly average total particle number concentrations measured by SMPS and CPC from April 4 - May 7, 2016.

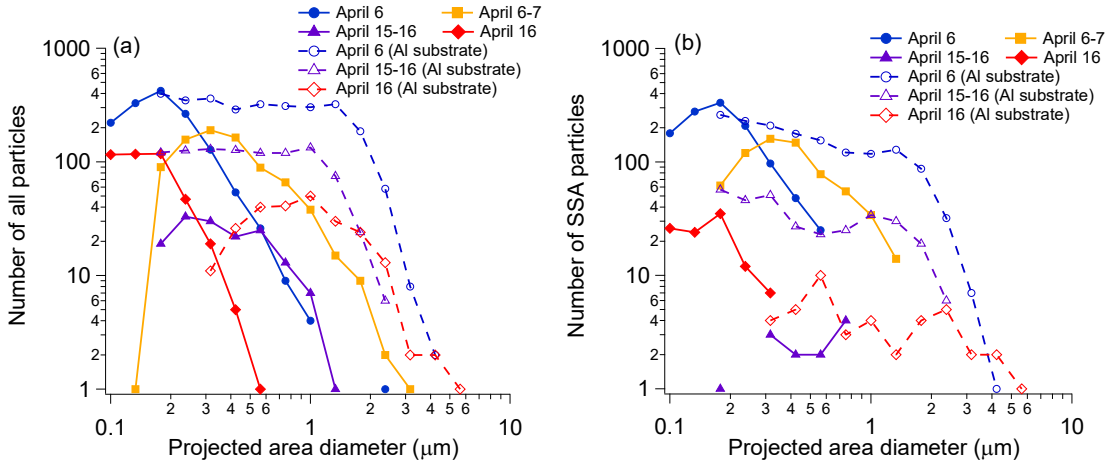

Figure S3. Number of (a) all particles and (b) sea salt aerosol particles identified, using CCSEM-EDX, across the 0.1-6 μm projected area diameter (d_{pa}) range (0.07-2.8 μm d_a impactor stages) for the April 6 07:00-19:00 AKDT, April 6 19:00 – April 7 07:00, April 15 19:00 – April 16 07:00, and April 16 08:00-20:00 samples. As detailed in the methods, 0.07-0.40 μm

160

d_a samples were collected on TEM grids, and 0.4-2.8 μm d_a particles were collected on aluminum (Al) substrate, as noted in legends.

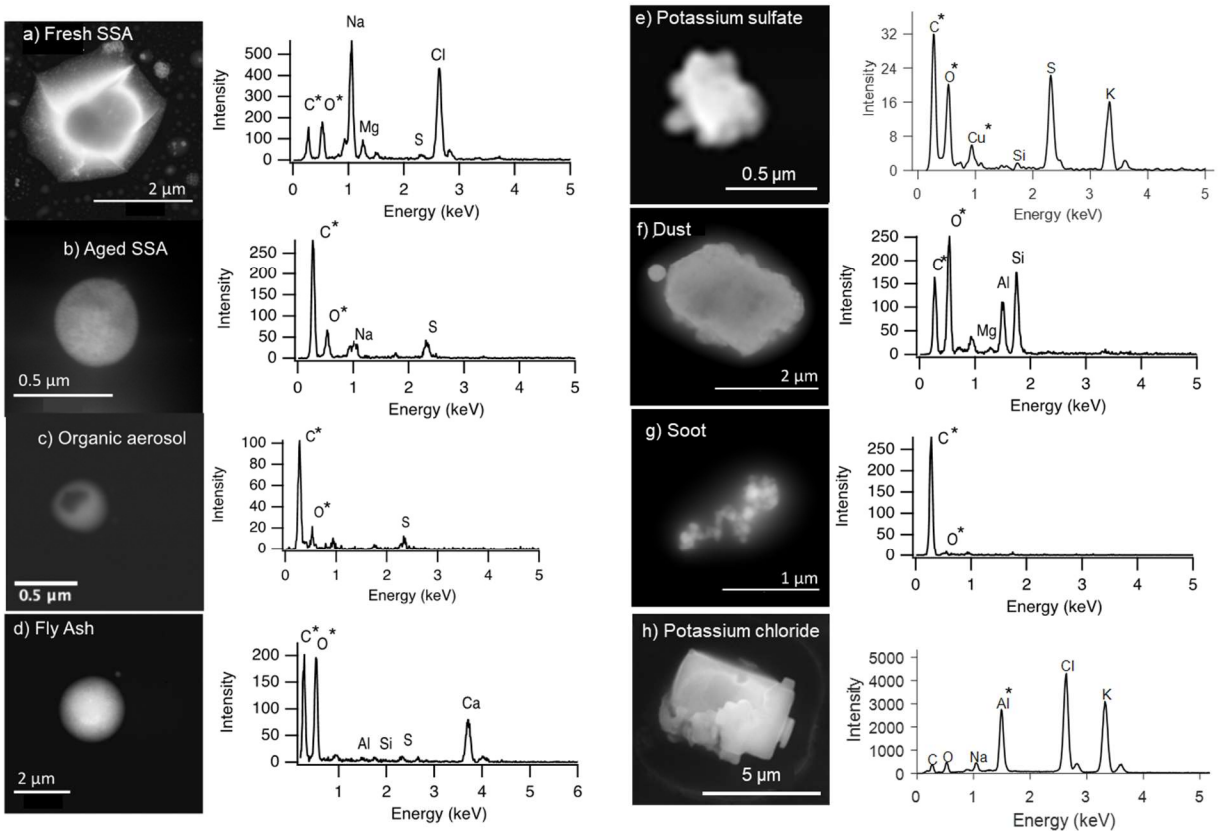

Figure S4. Representative SEM images and EDX spectra of the main particle types observed in April 6 and April 15-16 samples. The C, O, and Cu signals include contributions from the TEM grids in a-g, and the Al signal includes contributions from the aluminum substrate in h.

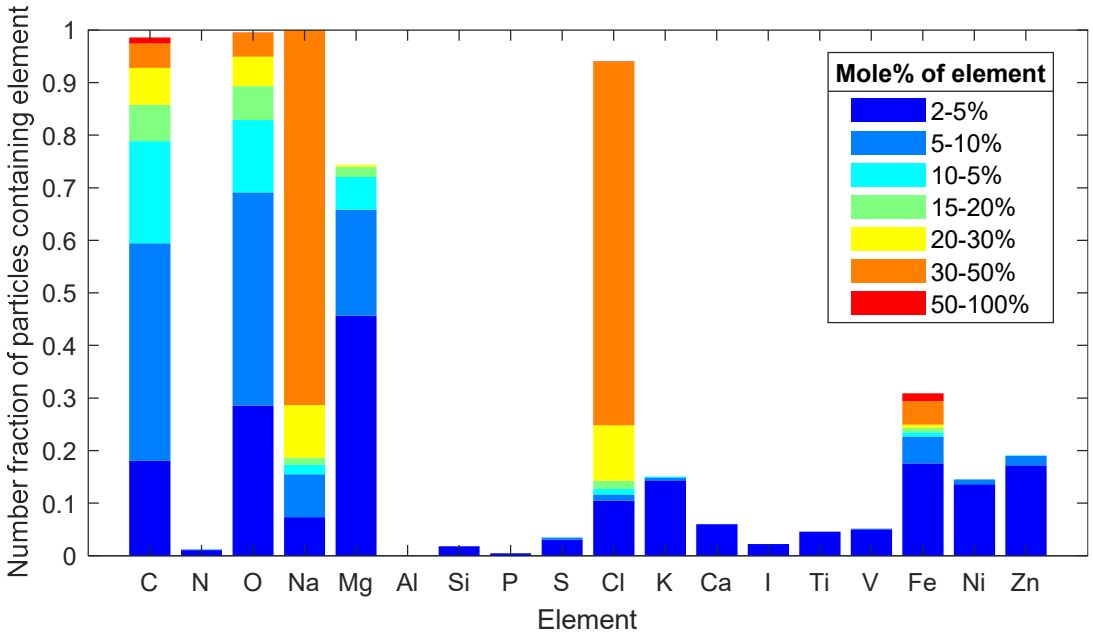

Figure S5. Digital color histogram of individual 0.4-2.8 μm d_a fresh sea spray aerosol particles, collected on aluminum foil. The digital color histogram heights represent the number fractions of individual sea spray aerosol particles containing a specific element, while the colors represent the mole percentage of that element in that number fraction of particles. Aluminum was removed from the EDX spectra due to contributions from the aluminum foil substrate.